Polyhedron 30 (2011) 2704–2710

Contents lists available at SciVerse ScienceDirect

Polyhedron

journal homepage: www.elsevier.com/locate/poly

Photoactive building blocks for coordination complexes: Gilding 2,2′:6′,2″-terpyridine

Edwin C. Constable *, Catherine E. Housecroft *, Marzena K. Kocik, Jennifer A. Zampese

Department of Chemistry, University of Basel, Spitalstrasse 51, 4056 Basel, Switzerland

ARTICLE INFO

Article history:
Received 14 June 2011
Accepted 1 August 2011
Available online 5 August 2011

Keywords:
Gold(I)
2,2′:6′,2″-Terpyridine
Phosphane
Alkyne
Photophysics

ABSTRACT

The alkyne unit of 4′-ethynyl-2,2′:6′,2″-terpyridine has been functionalized with Ph_3PAu, $(2\text{-tolyl})_3PAu$ or Au(dppe)Au units to produce compounds **1**–**3**, respectively. These derivatives have been characterized by electrospray mass spectrometry, solution ^1H and ^{13}C NMR, UV–Vis and emission spectroscopies, and single crystal X-ray diffraction. In the solid state, molecules of **1** or **2** pack with separated domains of tpy and R_3PAu units; the tpy units in **2** (but not **1**) exhibit face-to-face π-stacking. Compound **3** crystallizes as $2(\mathbf{3})\cdot CHCl_3$, and the folded conformation of the dppe backbone results in a short (2.9470(8) Å) aurophilic interaction. Folded molecule **3** captures $CHCl_3$, preventing intramolecular face-to-face π-interactions between the tpy units. In CH_2Cl_2 solution, **1**–**3** are emissive when excited between 230 and 300 nm, but over minutes when λ_{ex} = 230 nm, the emission bands decay as the compounds photodegrade.

1. Introduction

Gold(I) alkynyl complexes [1,2] containing gold atoms in linear coordination environments are popular building blocks for polymeric and macrocyclic organometallic assemblies [3–12]. The luminescent properties of gold(I) species [13,14] and the ease of synthesis of gold(I) alkynyls make them attractive candidates for derivatization of other metal-binding domains such as pyridine [15–19], 2,2′-bipyridine (bpy) [16,20,21] and 2,2′:6′,2″-terpyridine (tpy) [21,22]. The combination of a luminescent gold(I) unit and a chelating ligand provides an approach to the design of metal ion sensors.

In gold(I) derivatives, aurophilic interactions (i.e. short Au···Au contact of around 3.00–3.20 Å) [23] are considered important in influencing their emissive behaviour [24–27]. Recently, we reported the solid-state structures of four bis(gold(I) phosphane)-decorated 4,4′-diethynyl-2,2′-bipyridines (Scheme 1) [20]. Changing the phosphane from PEt_3 to P^iPr_3 alters the packing, producing different polymeric chain motifs. In both, Au···Au contacts of less than 3.4 Å are observed. For the more sterically demanding PPh_3 and P(4-tolyl)$_3$ substituents, no short Au···Au contacts are present in the solid state. In CH_2Cl_2 solution, each compound (Scheme 1) is a dual emitter at room temperature. However, with $\lambda_{ex} \approx 238$ nm, the emission spectra decay quite rapidly at the expense of a new set of emission maxima, and we have proposed that this arises from cleavage of the Au–C_{alkyne} bond. We now turn our attention to tpy-based compounds in which the alkynyl substituent is directly attached to the 4′-position of the tpy domain. This is in contrast to previously reported systems in which the tpy and C≡C units are separated by an arene spacer [21,22].

2. Experimental

2.1. General procedures

^1H and ^{13}C NMR spectra were recorded on a Bruker DRX-500 NMR spectrometer with chemical shifts referenced to residual solvent peaks ($CHCl_3$ = δ 7.24 ppm, TMS = δ 0 ppm). ^{31}P NMR spectra were recorded using a Bruker DRX-400 NMR spectrometer and were referenced with respect to 85% H_3PO_4 = δ 0 ppm. Absorption spectra were recorded using a Varian-Cary 5000 spectrophotometer and emission spectra using a Shimadzu RF-5301 PC spectrofluorometer; excitation/emission slit widths were set at 3/3, 5/3, 3/3, and 5/5 for 4′-ethynyl-2,2′:6′,2″-terpyridine, **1**, **2** and **3**, respectively. Electrospray ionization (ESI) mass spectra were measured with a Bruker esquire 3000^{plus} mass spectrometer.

4′-Ethynyl-2,2′:6′,2″-terpyridine was prepared according to the literature procedure starting from 4′-[(trifluoromethylsulfonyl)oxy]-2,2′:6′,2″-terpyridine [28]. R_3PAuCl with R = Ph or 2-tolyl was prepared by a reported route [29] with a reaction temperature of −5 °C. Abbreviation: tht, tetrahydrothiophene.

2.2. {Au(4′-C≡Ctpy)}$_n$

The synthesis of {Au(4′-C≡Ctpy)}$_n$ was based on that described for {Au(4-C≡Cpy)}$_n$ [17]. 4′-Ethynyl-2,2′:6′,2″-terpyridine (50 mg,

* Corresponding author. Fax: +41 61 267 1018.
E-mail address: catherine.housecroft@unibas.ch (C.E. Housecroft).

0277-5387/$ - see front matter © 2011 Elsevier Ltd. All rights reserved.
doi:10.1016/j.poly.2011.08.001

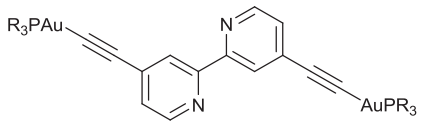

R = Et, ^{i}Pr, Ph, 4-tolyl

Scheme 1. Previously reported bis(gold(I) phosphane)-4,4′-diethynyl-2,2′-bipyridine compounds [20].

190 μmol), [(tht)AuCl] (63.5 mg, 190 μmol) and NaOAc (77.9 mg, 950 μmol) were added to a mixture of THF (5 cm^3) and MeOH (5 cm^3) under argon and with light excluded. The reaction mixture was stirred for 6–12 h after which time a pale yellow precipitate was obtained. This was collected by filtration and washed with MeOH. {Au(4′-C≡Ctpy)}$_n$ was isolated as yellow solid (72 mg, 159 μmol, ca. 82%) and was used without further purification.

2.3. Compound **1**

Ph_3PAuCl (38 mg, 78 μmol), 4′-ethynyl-2,2′:6′,2″-terpyridine (20 mg, 78 μmol), CuI (0.7 mg, 4 μmol) were dissolved in CH_2Cl_2 (8 cm^3) and MeOH (2 cm^3). NaOAc (13 mg, 156 μmol) was then added, and the reaction mixture stirred at room temperature in the dark for 12–16 h. It was then filtered and the solvent removed from the filtrate *in vacuo*. The crude material was purified by preparative plate chromatography in the dark (Al_2O_3, CH_2Cl_2). **1** was isolated as a white solid (39.3 mg, 55.3 μmol, 70.7%). ^{1}H NMR (500 MHz, $CDCl_3$) δ/ppm 8.66 (d, J = 4.0 Hz, 2H, H^{A6}), 8.54 (d, J = 8.1 Hz, 2H, H^{A3}), 8.52 (s, 2H, H^{B3}), 7.80 (td, J = 7.8, 1.7 Hz, 2H, H^{A4}), 7.54 (m, 6H, $H^{C2/C3}$), 7.49 (m, 3H, H^{C4}), 7.45 (m, 6H, $H^{C2/C3}$), 7.29 (m, 2H, H^{A5}). ^{13}C NMR (126 MHz, $CDCl_3$) δ/ppm 156.5 (C^{A2}), 155.4 (C^{B2}), 149.4 (C^{A6}), 136.8 (C^{A4}), 135.3 (C^{B4}), 134.5 (d, J_{PC} = 14 Hz, $C^{C2/C3}$), 131.8 (d, J_{PC} = 2 Hz, C^{C4}), 129.6 (d, J_{PC} = 56 Hz, C^{C1}), 129.4 (d, J_{PC} = 11 Hz, $C^{C2/C3}$), 124.3 (C^{B3}), 123.7 (C^{A5}), 121.3 (C^{A3}), 102.3 (poorly resolved, *C*≡CAu), signal for C≡*C*Au not observed. ^{31}P NMR (162 MHz, $CDCl_3$) δ/ppm 42.4. UV–Vis λ_{max}/nm (CH_2Cl_2) 229 (ε/dm^3 mol^{-1} cm^{-1} 53 000), 244 (50 000), 277 (54 000), 289 (62 000), 319 (9000), 331 (6000). Emission (CH_2Cl_2, λ_{exc} = 244 nm) λ_{em}/nm 339, 355. ESI MS (CH_2Cl_2/MeOH) *m/z* 1174.4 $[M+AuPPh_3]^+$ (calc. 1174.2), 716.3 $[M+H]^+$ (base peak, calc. 716.2). *Anal.* Calc. for $C_{35}H_{25}AuN_3P$: C, 58.75; H, 3.52; N, 5.87. Found: C, 58.55; H, 3.72; N, 5.92%.

2.4. Compound **2**

The method was as for **1**, starting with (2-tolyl)$_3$PAuCl (42 mg, 78 μmol), 4′-ethynyl-2,2′:6′,2″-terpyridine (20 mg, 78 μmol), NaOAc (13 mg, 156 μmol) and CuI (0.7 mg, 4 μmol). Compound **2** was isolated as a white solid (36.2 mg, 47.8 μmol, 61.6%). ^{1}H NMR (500 MHz, $CDCl_3$) δ/ppm 8.68 (dd, J = 4.6, 0.8 Hz, 2H, H^{A6}), 8.53 (d, J = 7.9 Hz, 2H, H^{A3}), 8.48 (s, 2H, H^{B3}), 7.79 (td, J = 7.7, 1.8 Hz, 2H, H^{A4}), 7.44 (t, J = 7.5 Hz, 3H, H^{C4}), 7.36 (m, 3H, H^{C3}), 7.26 (ddd, J = 7.4, 4.8, 1.0 Hz, 2H, H^{A5}), 7.17 (t, J = 7.6 Hz, 3H, H^{C5}), 6.93 (dd, J_{PH} = 12.2 Hz, J_{HH} = 7.7 Hz, 3H, H^{C6}), 2.73 (s, 9H, H^{Me}). ^{13}C NMR (126 MHz, $CDCl_3$) δ/ppm 156.3 (C^{A2}), 155.1 (C^{B2}), 151.1 (C^{A6}), 149.1 (d, J_{PC} = 13 Hz, C^{C2}), 136.6 (C^{A4}), 135.4 (C^{B4}), 133.6 (d, J_{PC} = 8 Hz, C^{C6}), 132.2 (d, J_{PC} = 9 Hz, C^{C3}), 131.6 (d, J_{PC} = 2 Hz, C^{C4}), 126.6 (d, J_{PC} = 9 Hz, C^{C5}), 126.2 (d, J_{PC} = 55 Hz, C^{C1}), 124.0 (C^{B3}), 123.5 (C^{A5}), 121.1 (C^{A3}), 102.4 (d, J_{PC} = 26.6 Hz, *C*≡CAu), 23.7 (d, J = 11 Hz, C^{Me}), signal for C≡*C*Au not observed. ^{31}P NMR (162 MHz, $CDCl_3$) δ/ppm 24.3. UV–Vis λ_{max}/nm (CH_2Cl_2), 251 (ε/dm^3 mol^{-1} cm^{-1} 53 000), 280 (59 000), 288 (64 000), 318 (9000), 332 (6000). Emission (CH_2Cl_2, λ_{exc} = 252 nm) λ_{em}/nm 341, 354. ESI MS (CH_2Cl_2/MeOH) *m/z* 1258.5 $[M+AuP(tolyl)_3]^+$ (calc. 1258.3), 805.2 $[Au\{P(tolyl)_3\}_2]^+$ (calc. 805.2), 758.4 $[M+H]^+$ (base peak, calc. 758.2). *Anal.* Calc. for $C_{38}H_{31}AuN_3P{\cdot}H_2O$: C, 58.84; H, 4.29; N, 5.42. Found: C, 59.14; H, 4.11; N, 5.38%.

2.5. Compound **3**

Bis(diphenylphosphinoethane) (dppe, 22 mg, 55 μmol) and {Au(4′-C≡Ctpy)}$_n$ (50 mg, 110 μmol) were stirred in CH_2Cl_2 (10 cm^3) for 30–60 min. After this time, the solvent was evaporated *in vacuo* and the crude product was purified in the dark by preparative plate chromatography (Al_2O_3, CH_2Cl_2). Compound **3** was isolated as white solid (31.2 mg, 23.9 μmol, 43.4%). ^{1}H NMR (500 MHz, $CDCl_3$) δ/ppm 8.68 (d, J = 4.6 Hz, 4H, H^{A6}), 8.56 (d, J = 8.0 Hz, 4H, H^{A3}), 8.55 (s, 4H, H^{B3}), 7.82 (td, J = 7.8, 1.5 Hz, 4H, H^{A4}), 7.72 (m, 8H, H^{C2}), 7.52 (overlapping m, 12H, $H^{C3/C4}$), 7.38 (m, 4H, H^{A5}), 2.69 (s, 4H, H^a). ^{13}C NMR (126 MHz, $CDCl_3$) δ/ppm 156.2 (C^{A2}), 155.3 (C^{B2}), 149.2 (C^{A6}), 136.7 (C^{A4}), 135.0 (C^{B5}), 133.5 (C^{C2}), 132.3 (C^{C4}), 129.7 (t, J_{PC} = 6 Hz, C^{C3}), 124.0 (C^{B3}), 123.7 (C^{A5}), 121.2 (C^{A3}), 102.0 (poorly resolved, *C*≡CAu), 24.0 (J_{PC} = 17 Hz, C^a), signals for C^{C1} and C≡*C*Au not observed. ^{31}P NMR (162 MHz, $CDCl_3$) δ/ppm 40.6. UV–Vis λ_{max}/nm (CH_2Cl_2) 230 (ε/dm^3 mol^{-1} cm^{-1} 122 000), 239 (11 6000), 254 (100 000), 277 (136 000), 289 (156 000), 319 (26 000), 332 (19 000). Emission (CH_2Cl_2, λ_{exc} = 241 nm) λ_{em}/nm 341, 355. ESI MS (CH_2Cl_2) *m/z* 1305.8 $[M+H]^+$ (calc. 1305.3), 1048.6 $[Au(dppe)AuCCtpy]^+$ (calc. 1048.2), 993.7 $[(dppe)_2Au]^+$ (calc. 993.2). *Anal.* Calc. for $C_{60}H_{44}Au_2N_6P_2{\cdot}2H_2O$: C, 53.74; H, 3.61; N, 6.27. Found: C, 53.76; H, 3.41; N, 6.00.

2.6. Crystal structure determinations

Data were collected on a Stoe IPDS diffractometer and the data reduction, solution and refinement used Stoe IPDS software [30] and SHELXL97 [31]. ORTEP figures were drawn using Ortep-3 for Windows [32], and the structures were analysed using Mercury v. 2.4 [33,34].

2.7. Compound **1**

$C_{35}H_{25}AuN_3P$, M = 715.52, colourless plate, monoclinic, space group $P2_1/c$, a = 19.658(4), b = 8.3726(17), c = 17.853(4) Å, β = 105.39(3)°, U = 2833.0(10) Å^3, Z = 4, D_{calc} = 1.678 Mg m^{-3}, μ(Mo Kα) = 5.279 mm^{-1}, T = 173 K. Total 44 788 reflections, 5835 unique, R_{int} = 0.0979. Refinement of 5641 reflections (361 parameters) with $I > 2\sigma(I)$ converged at final R_1 = 0.0426 (R_1 all data = 0.0435), wR_2 = 0.1087 (wR_2 all data = 0.1098), Goodness-of-fit = 1.144.

2.8. Compound **2**

$C_{38}H_{31}AuN_3P$, M = 757.60, colourless plate, triclinic, space group $P\bar{1}$, a = 9.2574(9), b = 17.6618(19), c = 19.504(2) Å, α = 107.172(8)°, β = 96.023(8)°, γ = 91.372(8)°, U = 3024.9(5) Å^3, Z = 4, D_{calc} = 1.664 Mg m^{-3}, μ(Mo Kα) = 4.949 mm^{-1}, T = 173 K. Total 67 142 reflections, 12 533 unique, R_{int} = 0.1018. Refinement of 11 198 reflections (782 parameters) with $I > 2\sigma(I)$ converged at final R_1 = 0.0491 (R_1 all data = 0.0537), wR_2 = 0.1379 (wR_2 all data = 0.1417), Goodness-of-fit = 1.182.

2.9. Compound 2(**3**)·$CHCl_3$

$C_{121}H_{89}Au_4Cl_3N_{12}P_4$, M = 2729.16, colourless needle, monoclinic, space group Pc, a = 10.389(2), b = 17.482(4), c = 15.652(3) Å, β = 98.53(3)°, U = 2811.2(10) Å^3, Z = 1, D_{calc} = 1.612 Mg m^{-3}, μ (Mo Kα) = 5.384 mm^{-1}, T = 173 K. Total 49 946 reflections, 10 592 unique, R_{int} = 0.1933. Refinement of 9643 reflections (669 parameters) with $I > 2\sigma(I)$ converged at final R_1 = 0.0625 (R_1 all

data = 0.0704), wR_2 = 0.1525 (wR_2 all data = 0.1591), Goodness-of-fit = 1.075.

3. Results and discussion

3.1. Synthesis and characterization of compounds 1 and 2

We have previously shown that coupling of 4,4′-diethynyl-2,2′-bipyridine and R_3PAuCl in the presence of diisopropylamine and CuI yields gold(I) phosphane-derivatized bpy ligands [20]. When this methodology was extended to the synthesis of gold(I) phosphane derivatives of 4′-ethynyl-2,2′:6′,2″-terpyridine, we found that it was more convenient to replace the organic base by NaOAc. Treatment of 4′-ethynyl-2,2′:6′,2″-terpyridine with R_3PAuCl (R = Ph or 2-tolyl) in a mixture of MeOH and CH_2Cl_2 in the presence of CuI and an excess of NaOAc resulted in the formation, after workup, of white solids **1** and **2**. In the ESI mass spectrum of **1**, peaks at *m/z* 1174.4 and 716.3 were assigned to $[M+AuPPh_3]^+$ and $[M+H]^+$. For **2**, the mass spectrum exhibited peaks at *m/z* 1258.5, 805.2 and 758.4, consistent with the ions $[M+AuP(tolyl)_3]^+$, $[Au\{P(tolyl)_3\}_2]^+$ and $[M+H]^+$, respectively. All isotope patterns were in accord with those simulated.

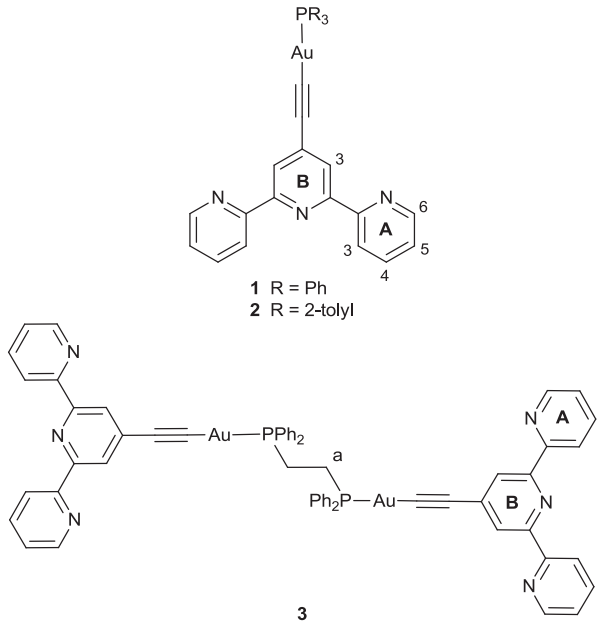

Scheme 2. Structures of compounds **1**–**3** with numbering schemes for NMR spectroscopic assignments. Phenyl and 2-tolyl rings are labelled C.

For each of compounds **1** and **2**, the ^{31}P NMR spectrum showed one singlet (δ 42.4 and 24.3 ppm, respectively, in $CDCl_3$) shifted to higher frequency with respect to the corresponding R_3PAuCl (δ 30.2 and 5.2, respectively, in $CDCl_3$). The signals in the solution ^1H and ^{13}C NMR spectra of **1** and **2** were assigned using COSY, DEPT, HMQC and HMBC techniques, and were consistent with the presence of a single tpy environment in each compound. In the ^{13}C NMR spectrum of **2**, a doublet at δ 102.4 ppm (J_{PC} = 26.6 Hz) [35] was assigned to C≡CAu, and this was confirmed by the observation of a cross-peak between this resonance and that of proton H^{B3} (see Scheme 2 for labelling). For **1**, the HMBC spectrum exhibited a cross-peak between the signal for H^{B3} and a poorly resolved signal at δ 102.3 ppm, and the latter was assigned to alkyne carbon C≡CAu. The resonance for the second alkyne ^{13}C nucleus was not observed in either **1** or **2**, a feature that we have also reported for gold(I) phosphane 4,4′-diethynyl-2,2′-bipyridine derivatives [20].

The structures of **1** and **2** were confirmed by single crystal X-ray diffraction. Suitable crystals were grown by slow diffusion of Et_2O into CH_2Cl_2/toluene solutions of the compounds. Compound **1** (Fig. 1) crystallizes in the $P2_1/c$ space group, while **2** (Fig. 2) crystallizes in space group $P\bar{1}$ with two independent molecules in the asymmetric unit. The structural features of **1** and **2** are similar. The tpy unit adopts the anticipated *trans,trans*-configuration and is essentially planar. The angles between the least squares planes of the pyridine rings containing N1/N2 and N2/N3 are 12.5(2)° and 3.4(2)° in **1**, 2.6(3)° and 15.5(3)° in molecule A of **2**, and 7.8(3)° and 3.9(3)° in molecule B of **2**. The C8–C16–C17–Au1–P1 linkage is close to linear in each compound (see captions to Figs. 1 and 2).

Fig. 3 illustrates the packing of molecules of **1** in the crystal lattice. The molecules are organised to give sheets of either tpy or Ph_3PAu domains. Alkyne atom C17 exhibits short contacts to two CH_{phenyl} units, one in each of two adjacent molecules ($C17\cdots H27a^{i}C27^{i}$ = 2.67 Å, $C17\cdots H32a^{ii}C32^{ii}$ = 2.90 Å, symmetry codes i = $-x$, $^1/_2 + y$, $^1/_2 - z$; ii = x, $1 + y$, z). There are no face-to-face π-interactions between adjacent tpy units. In contrast, the tpy units in neighbouring molecules of **2** are π-stacked (Fig. 4); tpy rings containing atoms N1a and N2a lie over those with $N1a^{i}$ and $N2a^{i}$ (symmetry code i = $3 - x$, $2 - y$, $2 - z$) with an optimal slipped arrangement and a separation of 3.4 Å. Similarly, the rings containing N1b and N2b are stacked over those containing $N1b^{ii}$ and $N2b^{ii}$ (symmetry code ii = $1 - x$, $2 - y$, $1 - z$) at a separation of 3.5 Å. The tpy domains extend into layers which lie in the *ac* plane, and consecutive tpy-sheets are separated by sheets of interlocked $P(2\text{-tolyl})_3$ units (Fig. 4).

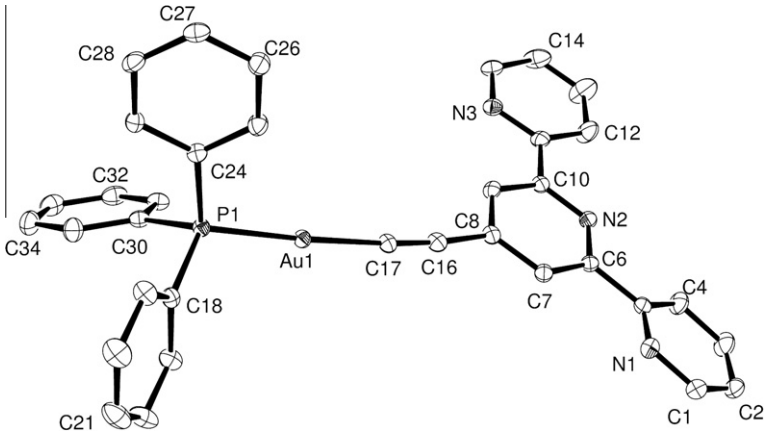

Fig. 1. Structure of compound **1** (ellipsoids plotted at 30% probability level; H atoms omitted). Selected bond parameters: Au1–C17 = 2.003(4), Au1–P1 = 2.2742(10), P1–C24 = 1.816(4), P1–C30 = 1.807(4), P1–C18 = 1.815(4), C16–C17 = 1.195(6) Å; C17–Au1–P1 = 176.93(11)°, C16–C17–Au1 = 176.1(4)°, C17–C16–C8 = 172.8(4)°.

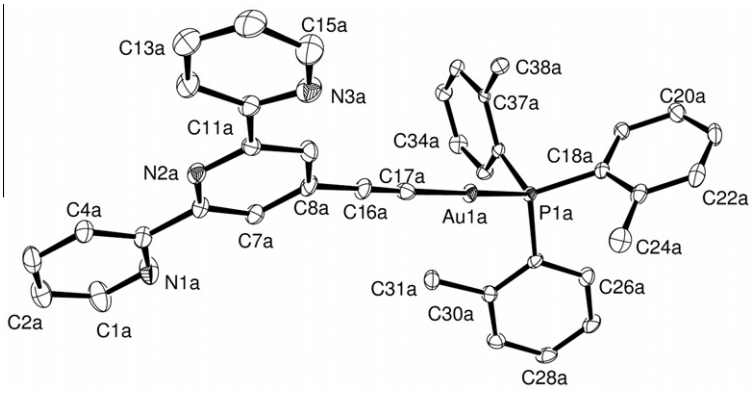

Fig. 2. One of the two independent molecules (molecule A) of **2** (ellipsoids plotted at 40% probability level; H atoms omitted). Selected bond parameters: Au1a–C17a = 1.996(6), Au1a–P1a = 2.2859(14), P1a–C18a = 1.815(5), P1a–C25a = 1.825(5), P1a–C32a = 1.830(6), C16a–C17a = 1.187(8) Å; C17a–Au1a–P1a = 172.31(19)°, C16a–C17a–Au1a = 175.7(6)°, C17a–C16a–C8a = 178.8(8)°. Bond parameters for the second independent molecule (molecule B) are similar.

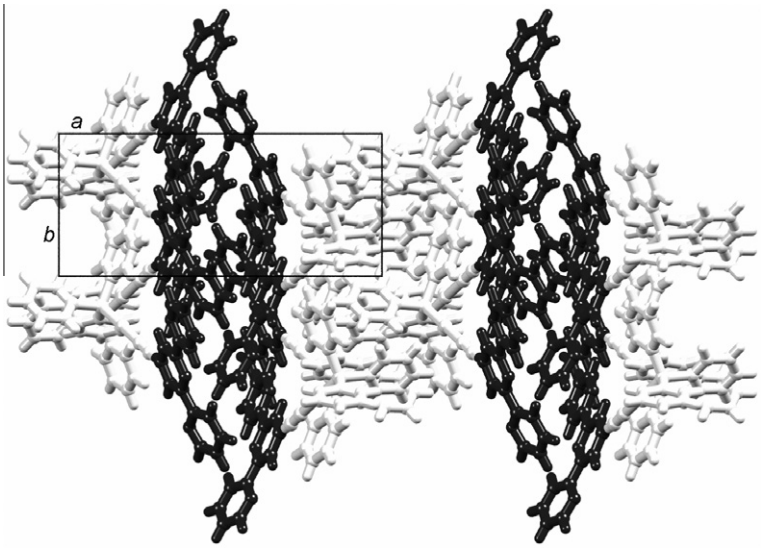

Fig. 3. View down the crystallographic *c* axis showing the packing of molecules of **1** into domains of tpy units (two domains shown) and Ph_3PAu units (three domains shown).

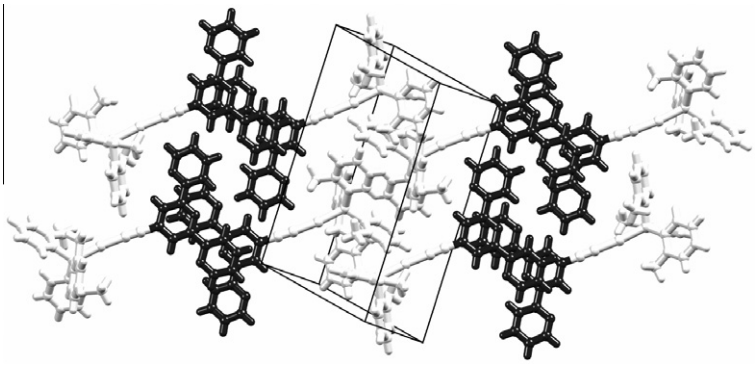

Fig. 4. Packing of molecules of **2** involves π-stacked domains of tpy units (two domains shown) separated by domains of $(2\text{-tolyl})_3PAu$ units (three domains shown).

3.2. Synthesis and characterization of ***3***

During attempts to prepare compound **3** in a similar manner to **1** and **2**, we encountered difficulties with the purification of the product, and therefore turned to the use of $\{Au(4'\text{-}C{\equiv}Ctpy)\}_n$ as a precursor, following the strategy adopted by Ferrer et al. for the preparation of rod-like isonitrile derivatives from treatment of $CNC_6H_4O(O)CC_6H_4OC_{10}H_{21}$-*p* with $\{Au(4\text{-}C{\equiv}Cpy)\}_n$ [17]. The polymer $\{Au(4'\text{-}C{\equiv}Ctpy)\}_n$ was prepared by reaction of 4′-ethynyl-2,2′:6′,2″-terpyridine with [(tht)AuCl] in the presence of NaOAc, and the yellow solid obtained was used without purification. Treatment of $\{Au(4'\text{-}C{\equiv}Ctpy)\}_n$ with dppe in CH_2Cl_2 resulted, after

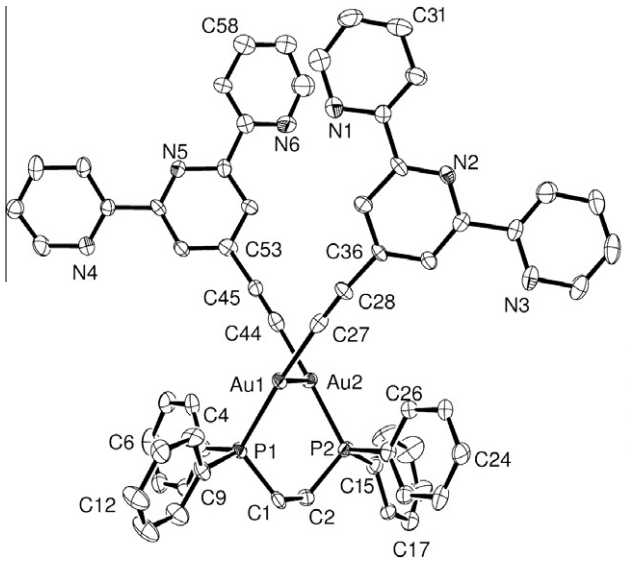

Fig. 5. Molecule of **3** in 2(**3**)·$CHCl_3$ (ellipsoids plotted at 30% probability level; H atoms omitted). Selected bond parameters: Au1–Au2 = 2.9470(8), Au1–C27 = 2.015(16), Au1–P1 = 2.287(3), Au2–C44 = 2.019(19), Au2–P2 = 2.272(4), P1–C1 = 1.806(17), P1–C3 = 1.815(14), P1–C9 = 1.827(17), P2–C21 = 1.797(14), P2–C15 = 1.811(16), P2–C2 = 1.830(16), C27–C28 = 1.18(2), C44–C45 = 1.18(2), C28–C36 = 1.453(17), C45–C53 = 1.46(2) Å; C27–Au1–P1 = 173.8(4)°, C27–Au1–Au2 = 96.0(4)°, P1–Au1–Au2 = 87.54(9)°, C44–Au2–P2 = 176.8(4)°, C44–Au2–Au1 = 93.5(5)°, P2–Au2–Au1 = 88.37(10)°, C28–C27–Au1 = 174.2(13)°, C27–C28–C36 = 171.0(17)°, C45–C44–Au2 = 176.4(15)°, C44–C45–C53 = 175.9(17)°.

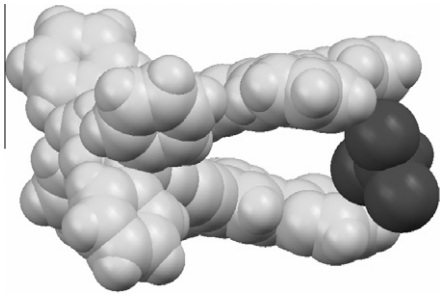

Fig. 6. Space-filling diagram to show the sandwich effect of the two tpy domains around the $CHCl_3$ solvent molecule.

work up, in the isolation of **3** in moderate yield. In the ESI mass spectrum, the highest mass peak envelope at *m/z* 1305.8 was assigned to $[M+H]^+$. Additional peaks were observed at *m/z* 1048.6 and 993.7 arising from the ions $[Au(dppe)AuCCtpy]^+$ and $[(dppe)_2Au]^+$. The solution ^{31}P NMR spectrum exhibited one singlet at δ 40.6 ppm, consistent with a symmetrical environment for the dppe ligand. This was supported by the observation of one signal for the methylene groups in each of the ^1H and ^{13}C NMR spectra, and the spectra were also consistent with the presence of one tpy environment; the resonances were assigned using COSY, DEPT, HMQC and HMBC methods. As for **1** and **2**, the signal for C≡CAu was not observed, while the second alkyne carbon gave rise to a poorly resolved signal at δ 102.0 ppm. This assignment was confirmed by a cross-peak in the HMBC spectrum to the resonance for proton H^{B3}.

Single crystals of 2(**3**)·$CHCl_3$ were grown by slow diffusion of Et_2O into a $CH_2Cl_2/CHCl_3$/toluene solution of **3**, and X-ray diffraction structure determination confirmed the molecular structure shown in Fig. 5. The two gold(I) centres are in close contact with a separation of 2.9470(8) Å, consistent with an aurophilic interaction [36,37]. In theory, the folded conformation of **3** could have resulted in face-to-face π-interactions between the two tpy units, but as Fig. 6 illustrates, this is prevented by the guest chloroform molecule. Closest contacts are C32H32a···Cl2 = 3.27 Å and C60H60a···Cl3 = 3.61 Å.

The packing of molecules of **3** in 2(**3**)·$CHCl_3$ comprises two assembly motifs. The first consists of ribbons which run parallel to the *a*-axis and are generated by face-to-face π-interactions; two out of three pyridine rings are involved (separation of rings containing N4 and $N2^i$ = 3.3 Å, and of rings with N5 and $N3^i$ = 3.5 Å, symmetry code i = 1 + *x*, *y*, *z*), leaving the third pyridine ring protruding from one side of the ribbon (Fig. 7a). The ribbons are arranged in a herringbone fashion (Fig. 7b), the assembly being supported by CH···C_{alkyne} and CH···N^i contacts, the latter involving the non-π-stacked pyridine ring: C58H58a···$C45^i$ = 2.86 Å, C31H31a···$N5^{ii}$ = 2.74 Å, symmetry codes i = *x*, 2 − *y*, $^1/_2$ + *z*, ii = −1 + *x*, 2 − *y*, $-^1/_2$ + *z*. This leads to short, repulsive H···H contacts (C59H59a···$H20a^iC20^i$ = 2.32 Å).

3.3. Photophysical properties

The electronic absorption spectrum of a CH_2Cl_2 solution of 4′-ethynyl-2,2′:6′,2″-terpyridine exhibits bands at 241 and 280 nm and a low energy tail with broad, low intensity maxima at 317 and 329 nm (Fig. 8). The absorptions arise from alkyne and tpy $\pi^* \leftarrow \pi$ and $\pi^* \leftarrow n$ transitions. An increase in ε_{max} is observed on going from 4′-ethynyl-2,2′:6′,2″-terpyridine to each of compounds **1**, **2** and **3**, and the approximate doubling in the values of ε_{max} on going from **1** or **2** to compound **3** is consistent with the doubling of the number of tpy and alkyne units per molecule. The pattern of absorptions in the region between 260 and 310 nm is similar for each of compounds **1**–**3**, with two maxmima at ca. 276 and 289 nm. Based on studies of related species [21,38–41] the transi-

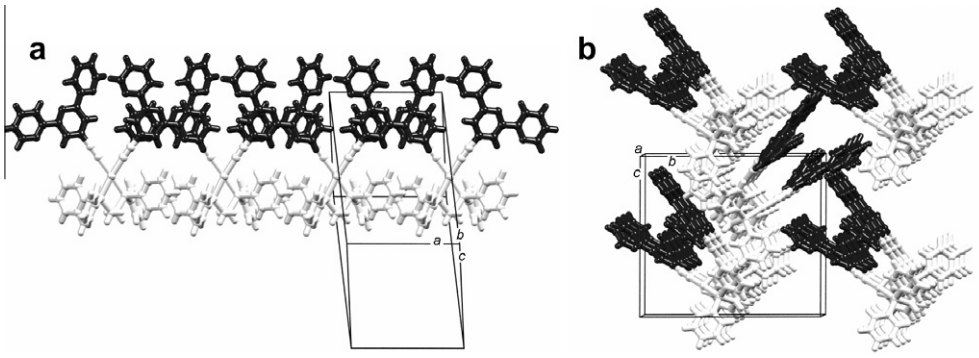

Fig. 7. (a) Assembly of a ribbon along the crystallographic *a* axis through π-stacking of tpy domains. (b) View down the *a* axis showing the herringbone arrangement of the ribbons.

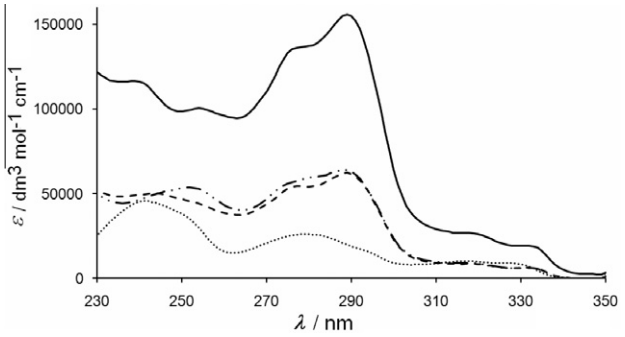

Fig. 8. Electronic absorption spectra of CH_2Cl_2 solutions of 4′-ethynyl-2,2′:6′,2″-terpyridine (·····), **1** (—), **2** (– ·· –) and **3** (–).

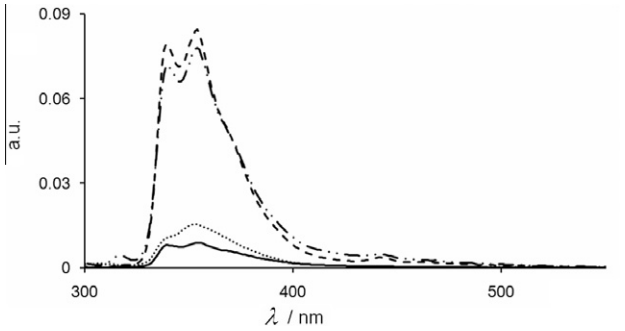

Fig. 9. Emission spectra for CH_2Cl_2 solutions of 4′-ethynyl-2,2′:6′,2″-terpyridine (·····), **1** (—), **2** (– ·· –) and **3** (–) ($\lambda_{ex} \sim 289$ nm). Concentrations: 4′-ethynyl-2,2′:6′,2″-terpyridine, 1.2×10^{-5}; **1**, 8.4×10^{-6}; **2**, 8.6×10^{-7}; **3**, 4.3×10^{-7} mol dm^{-3}. Slit widths: see Section 2.

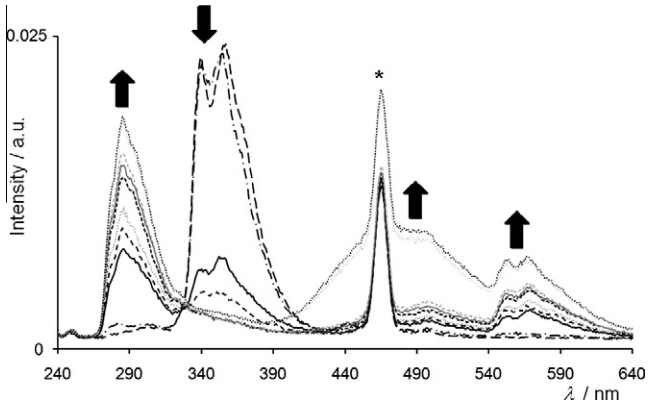

Fig. 10. Emission spectrum of **1** recorded approximately each minute over a 10 min period (λ_{ex} = 230 nm; *first harmonic).

tions that give rise to the observed absorption spectra are most likely to be tpy/alkyne $\pi^* \leftarrow \pi$ with Au orbital participation.

When irradiated at 289 nm, 4′-ethynyl-2,2′:6′,2″-terpyridine emits at 351 nm with a high energy shoulder at 342 nm. On going to compounds **1**–**3** (λ_{ex} = 289 nm), the emission is resolved into two clearly defined bands at 338 and 352 nm for **1**, 339 and 353 for **2**, and 342 and 352 nm for **3** (Fig. 9). Excitation spectra confirm that the origins of these emissions are the broad absorptions between 230 and 300 nm shown in Fig. 8.

Measurements of the emission spectra for compounds **1**–**3** were repeated approximately every minute over a period of 10–15 min with λ_{ex} = 230 nm. The emission bands (Fig. 9) decayed

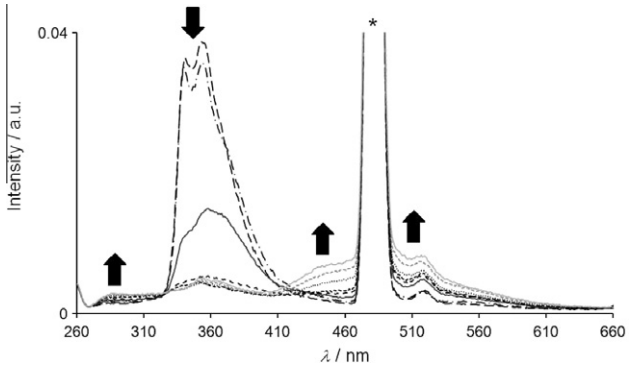

Fig. 11. Emission spectrum of **3** recorded approximately each minute over an 8 min period (λ_{ex} = 239 nm; *first harmonic).

and new bands grew in (Fig. 10). Compared to those for **1**, the new emission bands appeared at similar wavelengths for **2**, suggesting that the photodegradation products were related. The changes in emission spectra of **3** as a function of time are depicted in Fig. 11. The broad band that grows in between 410 and 560 nm is consistent with one of the broad emissions observed upon degradation of **1** and **2**, but the strong emission observed at 280 nm as **1** degrades (Fig. 10) is almost completely quenched in **3** (Fig. 11). When λ_{ex} was at wavelengths higher than 230 nm, photodecay was much slower. We have not been able to determine the identities of the photodegradation products, but note that comparable decay and growth of bands in the emission spectra of gold(I) phosphane derivatives of 4,4′-diethynyl-2,2′-bipyridine are observed over time [20]. In particular, as **1** decays, the emission centred around 570 nm (Fig. 10) matches that observed for the photodecay of 4,4′-($R_3PAuC{\equiv}C)_2$-2,2′-bipyridine (R = Ph or 4-tolyl) and we suggested [20] that this arises from the formation of small gold nanoclusters [42].

4. Conclusions

Functionalization of 4′-ethynyl-2,2′:6′,2″-terpyridine with Ph_3PAu, $(2\text{-tolyl})_3PAu$ or Au(dppe)Au units leads to the compounds **1**–**3** respectively which have been characterized spectroscopically in solution and by single crystal X-ray diffraction studies. In the solid state, molecules of **1** or **2** are arranged in domains of tpy or R_3PAu units; in **2**, the tpy units engage in face-to-face π-stacking, but analogous interactions are not observed in **1**. Compound **3** crystallizes as 2(**3**)·$CHCl_3$; the dppe backbone adopts a folded conformation, bringing the two gold(I) centres within 2.9470(8) Å of one another, but π-stacking of the tpy domains is prevented by a guested $CHCl_3$ molecule. Compounds **1**–**3** are emissive in CH_2Cl_2 solution, but over a period of minutes when λ_{ex} = 230 nm, the emission bands decay, consistent with the photodegradation of the compounds.

Acknowledgements

We thank the Swiss National Science Foundation and the University of Basel for financial support.

Appendix A. Supplementary data

CCDC 829106, 829107 and 829108 contain the supplementary crystallographic data for **2** and **4**. These data can be obtained free of charge via http://www.ccdc.cam.ac.uk/conts/retrieving.html, or from the Cambridge Crystallographic Data Centre, 12 Union Road,

Cambridge CB2 1EZ, UK; fax: (+44) 1223-336-033; or e-mail: deposit@ccdc.cam.ac.uk.

References

[1] H. Schmidbaur, A. Schier, in: R.H. Crabtree, D.M.P. Mingos (Eds.), Comprehensive Organometallic Chemistry III, vol. 2, Elsevier, Oxford, 2007, p. 251 (Chapter 5).
[2] N.J. Long, C.K. Williams, Angew. Chem., Int. Ed. 42 (2003) 2586.
[3] M.J. Irwin, J.J. Vittal, R.J. Puddephatt, Organometallics 16 (1997) 3541.
[4] J. Vicente, M.T. Chicote, M.D. Abrisqueta, M.M. Alvarez-Falcón, J. Organomet. Chem. 663 (2002) 40.
[5] F. Mohr, D.J. Eisler, C.P. McArdle, K. Atieh, M.C. Jennings, R.J. Puddephatt, J. Organomet. Chem. 670 (2003) 27.
[6] G. Hogarth, M.M. Alvarez-Falcón, Inorg. Chim. Acta 358 (2005) 1386.
[7] J. Vicente, M.-T. Chicote, M.M. Alvarez-Falcón, P.G. Jones, Organometallics 24 (2005) 2764.
[8] M.-A. MacDonald, R.J. Puddephatt, G.P.A. Yapp, Organometallics 19 (2000) 2194.
[9] W.J. Hunks, M.-A. MacDonald, M.C. Jennings, R.J. Puddephatt, Organometallics 19 (2000) 5063.
[10] F. Mohr, R.J. Puddephatt, J. Organomet. Chem. 689 (2004) 374.
[11] N.C. Habermehl, D.J. Eisler, C.W. Kirby, N.L.-S. Yue, R.J. Puddephatt, Organometallics 25 (2006) 2921.
[12] H.-S. Tang, N. Zhu, V.W.-W. Yam, Organometallics 26 (2007) 22.
[13] E.R.T. Tiekink, J.-G. Kang, Coord. Chem. Rev. 253 (2009) 1627.
[14] V.W.-W. Yam, E.C.-C. Cheng, Chem. Soc. Rev. 37 (2008) 1806.
[15] J. Vicente, M.T. Chicote, M.M. Alvarez-Falcón, Organometallics 23 (2004) 5707.
[16] R. Packheiser, A. Jakob, P. Ecorchard, B. Walfort, H. Lang, Organometallics 27 (2008) 1214.
[17] M. Ferrer, M. Mounir, L. Rodríguez, O. Rossell, S. Coco, P. Gómez-Sal, A. Martín, J. Organomet. Chem. 690 (2005) 2200.
[18] H.-Y. Chao, W. Lu, M.C.W. Chan, C.-M. Che, K.-K. Cheung, N. Zhu, J. Am. Chem. Soc. 124 (2002) 14696.
[19] M. Ferrer, L. Rodríguez, O. Rossell, F. Pina, J.C. Lima, M.F. Bardia, X. Solans, J. Organomet. Chem. 678 (2003) 82.
[20] E.C. Constable, C.E. Housecroft, M.K. Kocik, M. Neuburger, S. Schaffner, J.A. Zampese, Eur. J. Inorg. Chem. (2009) 4710.
[21] J. Vicente, J. Gil-Rubio, N. Barquero, P.G. Jones, D. Bautista, Organometallics 27 (2008) 646.
[22] X.-L. Li, K.-J. Zhang, J.-J. Li, X.-X. Cheng, Z.-N. Chen, Eur. J. Inorg. Chem. (2010) 3449.
[23] H. Schmidbaur, Chem. Soc. Rev. 24 (1995) 391.
[24] C.-M. Che, S.-W. Lai, in: F. Mohr (Ed.), Gold Chemistry, Wiley-VCH, 2009, p. 249.
[25] See for example: P. Li, B. Ahrens, K.-H. Choi, M.S. Khan, P.R. Raithby, P.J. Wilson, W.-Y. Wong, CrystEngComm 4 (2002) 405.
[26] See for example: C. King, J.-C. Wang, N.I. Khan, J.P. Fackler Jr., Inorg. Chem. 28 (1989) 2145.
[27] See for example: C.-M. Che, H.-L. Kwong, V.W.-W. Yam, K.-C. Cho, Chem. Commun. (1989) 885.
[28] V. Grosshenny, F.M. Romero, R. Ziessel, J. Org. Chem. 62 (1997) 1491.
[29] M.I. Bruce, E. Horn, J.G. Matisons, M.R. Snow, Aust. J. Chem. 37 (1984) 1163.
[30] Stoe & Cie, IPDS Software v 1.26, Stoe & Cie, Darmstadt, Germany, 1996.
[31] G.M. Sheldrick, Acta Crystallogr., Sect. A 64 (2008) 112.
[32] L.J. Farrugia, J. Appl. Crystallogr. 30 (1997) 565.
[33] I.J. Bruno, J.C. Cole, P.R. Edgington, M.K. Kessler, C.F. Macrae, P. McCabe, J. Pearson, R. Taylor, Acta Crystallogr., Sect. B 58 (2002) 389.
[34] C.F. Macrae, I.J. Bruno, J.A. Chisholm, P.R. Edgington, P. McCabe, E. Pidcock, L. Rodriguez-Monge, R. Taylor, J. van de Streek, P.A. Wood, J. Appl. Crystallogr. 41 (2008) 466.
[35] E.C. Constable, C.E. Housecroft, M. Neuburger, S. Schaffner, E.J. Shardlow, Polyhedron 27 (2008) 65.
[36] F. Mendizabal, P. Pyykkö, N. Runeberg, Chem. Phys. Lett. 370 (2003) 733.
[37] P. Pyykkö, Angew. Chem., Int. Ed. 41 (2002) 3573.
[38] D. Li, X. Hong, C.M. Che, W.C. Lo, S.M. Peng, J. Chem. Soc., Dalton Trans. (1993) 2929.
[39] M. Ferrer, A. Gutierrez, L. Rodriguez, O. Rossell, J.C. Lima, M. Font-Bardia, X. Solans, Eur. J. Inorg. Chem. (2008) 2899.
[40] V.W.-W. Yam, S.W.-K. Choi, K.-K. Cheung, Organometallics 15 (1996) 1734.
[41] V.W.-W. Yam, S.W.-K. Choi, J. Chem. Soc., Dalton Trans. (1996) 4227.
[42] Y. Bao, C. Zhong, D.M. Vu, J.P. Temirov, R.B. Dyer, J.S. Martinez, J. Phys. Chem. C 111 (2007) 12194.